(2+1)-dimensional stochastic growth model and its application to some experimental observations

S. V. Ghaisas
Department of Electronic Science, University of Pune, Pune 411007, India
(Received 31 August 2000; revised manuscript received 25 January 2001; published 23 May 2001)

A $(2+1)$-dimensional stochastic growth model is proposed in order to understand various experimental observations at low temperature growth. The model includes step attached adatom hopping in the upward direction to provide a source of additional particle current. The flexibility obtained due to additional current control allows one to express most of the experimental observations within the framework of this model. It is argued that the time evolution exponent β for surface roughness is >0.5 only if upward hops are included. Simulations using this model are shown to be qualitatively consistent with the observations for homoepitaxial growth on Cu(100) and Ge(100) at different temperatures.

DOI: 10.1103/PhysRevE.63.062601 PACS number(s): 68.03.−g, 68.55.−a, 82.20.Fd

Epitaxial growth of films from vapor has been studied keenly over the years due to technological need and applications. Such growth is carried out mostly under conditions far removed from equilibrium. A variety of surface morphologies appears during the growth [1]. In particular, the growth of a moundlike structure on singular surfaces, referred to as growth instability, is one of the common modes into which a growing interface evolves. It has been studied experimentally [2–6], theoretically [7–11], and simulationally [12–15] over the past few years, with only partial success in understanding the phenomenon. The time evolution of mounds is characterized by two exponents β and n, where the height grows as $\sim t^{\beta}$ and the base as $\sim t^{n}$ [11]. Experimentally β is observed to vary in the range of 0.16 [4] to about 0.8 [2,5]. Most theories and simulations for low temperature growth predicted $\beta \leqslant 0.5$. In the present paper it is argued that theories and simulations allowing only in-plane hops and hops from upper to lower terraces (downward), predict $\beta \leqslant 0.5$. Higher values of β are possible *only* when hops from lower to upper terraces (upward) are allowed. In a $(1+1)$-dimensional model [16], on the vicinal surface a transient increase in $\beta > 0.5$ was reported. However, the asymptotic value of β is 0.5. This increase in β is related to a morphological transition from a stable structure to an unstable (grooved) structure [16]. Results of our model show that the asymptotic value of β can be >0.5 if upward hops are included. A cellular automata type model [12] is used in support of this argument. Although simulation results can qualitatively describe any experimental growth, we have chosen Cu(100) and Ge(100) growth results [2,3] for comparison. First we argue, assuming solid-on-solid (SOS) random growth under deposition noise as a reference, to show how different types of hops affect the width and hence β. Another argument, based on an analysis of the asymptotic current forms suitable for different types of hops, without noise, essentially leads to the same conclusions.

Consider a $(1+1)$-dimensional growing surface with an average height $\overline{h}$. The width at time t is measured as $w_2 = (1/N)\Sigma_i (h_i - \overline{h})^2$. Let an atom hop from site i to $i+1$. The resultant width $w_2' = (1/N)\Sigma_j' (h_j - \overline{h})^2 + (h_i - 1 - \overline{h})^2 + (h_{i+1} + 1 - \overline{h})^2$, where the primed sum indicates the exclusion of ith and $i+1$th terms from the summation. It can be seen that for downward hops $w_2' < w_2$, for in-plane hops $w_2' = w_2$, and for upward hops $w_2' > w_2$. The decrease (increase) in the width, due exclusively to downward (upward) hops at any given time, is proportional to $\langle h_{i+1} - h_i \rangle$, which is >0 for upward hops and <0 for downward hops. Thus change due to hops $\delta w_2 \sim \pm \langle |h_{i+1} - h_i| \rangle$, where the plus sign is for upward hops and the minus sign is for downward hops. This change is superimposed on the fluctuations developed due to the noise in the deposition. As long as the correlations developed are weak, $\langle |h_{i+1} - h_i| \rangle \sim t^{1/2}$. This will cause β to deviate from its value for random deposition. Hence we conclude that for downward (upward) hops, the exponent β must be $\leqslant 0.5$ ($\geqslant 0.5$). For in-plane hops, the width changes *only* under deposition noise; thus $\beta = 0.5$ in any dimension. Next we consider an analysis of current forms, representing currents due to different types of hops.

From the nature of the hops, it is clear that on an inclined substrate [17], downward hops produce a current in a direction opposite to that of the height gradient (downhill), while in-plane and upward hops produce a current in the direction of the gradient (uphill). Thus the total current is $\mathbf{j} = \mathbf{j}_d + \mathbf{j}_i + \mathbf{j}_u$, with d, i, and u the suffixes for downward, in-plane, and upward hop contributions. Consider the case when $\mathbf{j}_u = 0$ and $\mathbf{j}_i > \mathbf{j}_d$. In-plane hops generating $\mathbf{j}_i$ can be due to the step Ehrlich-Schwoebel barrier (SESB) [18] or due to the kink Ehrlich-Schowoebel barrier [19]. The in-plane hopping contribution is directly proportional to the avarage terrace width. Hence a suitable form that describes j_i asymptotically is $\mathbf{j}_i \sim (\mathbf{m}/m^2) - (1/m^3)\boldsymbol{\nabla}(m)$ where m is local slope [10]. The first term represents an average terrace width, and tends to zero as m increases. The second term arises due to the relative terrace width fluctuations, and is a stabilizing term. It can be shown, using the method described in Ref. [11], that for the above form $\beta = 0.5$ in all dimensions. In fact, for a surface relaxation of the form $\Delta^n m$, with $n \geqslant 2$, $\beta = 0.5$ in all dimensions [11]. This shows that when j_i dominates the growth, $\beta = 0.5$ asymptotically. Lower values of β are possible with slope selection [9,20].

Now consider $\mathbf{j}_u > \mathbf{j}_d + \mathbf{j}_i$. We model $\mathbf{j}_u$ as being due to the step attached adatoms that hop on the upper terrace of the same step. $\mathbf{j}_u$ depends on the average number of step edges that saturates for large m. Thus $\mathbf{j}_u \rightarrow$ a nonzero constant, for

large m. A suitable form in this limit is $j_u \sim m/|m|$. It is shown that for surface relaxation of the form $\Delta^n m$, with $n>1$, $\beta>0.5$ [11]. Thus the above arguments show that β can be greater than 0.5 only when upward hops dominate.

In the following a cellular automata type SOS model [12] is described that incorporates all three types of hops. These types of models are relatively efficient for computational purposes, compared to molecular dynamical or kinetic Monte Carlo like simulations. Various microscopic processes can be included in such models, and their effects on statistical properties can be examined. The condition of detailed balance is not satisfied in this model unless extra rules for hopping are invoked. Atoms are rained down randomly on a square lattice. Let $h(i,j)$ be the height at site (i,j), while $h(i',j')$ at (i',j') is a nearest neighbor (NN) site. The adatom relaxes instantly if N_n the number of NN's is zero or 1. If $N_n=0$ (isolated adatom), the adatom can relax by hopping to any of the four NN sites. For a downward hop $[h(i,j)>h(i',j')]$, we associate a weight p_1, while for the in-plane hop $[h(i,j)=h(i',j')]$ we use p_2. Using these weightings, the probabilities for hopping at each of the four sites are determined, and are distributed in an interval from 0 to 1. The destination site is determined by picking a random number between 0 and 1. The adatom is allowed up to n number of such hops. If it encounters $N_n>1$, no further hops are allowed. If the number n is exhausted, the adatom stays in the last acquired position. The Ehlrich-Schwoebel length $l_s=[(p2/p1)-1]$ [10] in the present model. If $N_n=1$ on deposition (step-attached adatom), the adatom can hop downward $[h(i,j)>h(i',j')]$ or upward $[h(i,j)<h(i',j')]$ with weightings p_3 and p_4, respectively. In-plane dissociation and edge diffusion is not allowed. The parameters p_is and n are qualitatively comparable with various rates in the Arrhenius form $\exp(-E/kT)$. This allows us to deduce qualitative effects of temperature on the parameters, and hence on the growth. In the same spirit we allow only a fraction q of the total encountered deposited step attached adatoms to relax, and a $1-q$ fraction of the isolated adatoms to relax. The parameter q accounts for the relative binding strengths of the step attached and isolated adatoms. Thus an increase in the temperature is realized qualitatively when $|p_1-p_2|$ and $|p_3-p_4|$ decrease from previous values, q increases toward 0.5, and hops n increase. In what follows, we have chosen a set of parameters to produce results that show similarities to the results obtained from the growth of Cu(100) and Ge(100). Given that the nature of these parameters is like fitting parameters, a direct comparison with different kinetic rates on the surfaces of Cu and Ge is not valid. However, the similarity between the simulated results and the experimental observations points to the relative strengths of different types of hops in the growth under comparison.

In order to compare with the experimental results, width w_2 and height- height correlations $G(\mathbf{r},t)$ and $\langle h_i h_j \rangle$ are computed, where $w_2=(1/N)\Sigma_i(h_i-\overline{h})\sim t^{2\beta}$ and $G(\mathbf{r},t)=(1/N)\Sigma_{\mathbf{r}'}[h(\mathbf{r}+\mathbf{r}',t)-h(\mathbf{r}',t)]^2$. The average mound size d is measured as the distance of first peak in $\langle h_i h_j \rangle$ from the origin, while $A=G^{1/2}(d/2,t)$ [2]. w_2 and A are related as

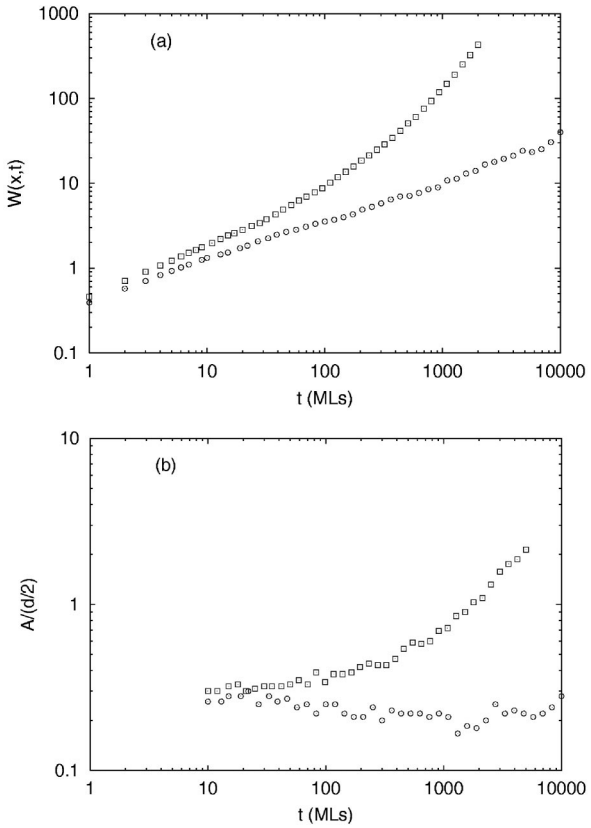

FIG. 1. (a) Plot of w_2 vs thickness for $p_1=0.02$, $p_2=1.0$, $p_3=2.0$, $p_4=1.0$, $q=0.2$, and $n=4$, (open circles), and for $p_1=0.04$, $p_2=1.0$, $p_3=2.0$, $p_4=1.2$, $q=0.4$, and $n=5$ (open squares). The upper curve is for higher temperature, while the lower one is for lower temperature. The substrate size used is $L=200$. (b) Plot of $A/(d/2)$ vs thickness for the set of parameters used in (a). Open circles are for lower temperature, and open squares are for higher temperature.

$A^2=2w_2$. The ratio $A/(d/2)$ is a measure of the average mound angle. The skewness $\sigma=w_3/w_2^{3/2}$ is measured, where $w_3=(1/N)\Sigma_i(h_i-\overline{h})^3$ [21].

Comparison with growth on Cu (100): Experimentally, β is measured during the growth on Cu(100) at two different temperatures, viz. 160 and 200 K, using the reflection high energy electron diffraction technique [3]. Measured values of β are 0.26 and 0.56 at 160 and 200 K, respectively, over a growth of 200 monolayers (ML). Figure 1(a) shows plots of w_2 vs t for two sets of parameters used to simulate the growth at different temperatures. Note that changes in the parameter values are consistent with changes in the ''temperature,'' as discussed earlier. The lower curve represents a roughness evolution at lower temperature, with a β value of 0.23 ± 0.03. The upper curve is for a higher temperature with a slowly increasing slope. The β value of 0.46 ± 0.4 is obtained in a thickness range from 50 to 400 ML. Note that there is a downward bias for isolated adatoms and an upward bias for step attached adatoms. Figure 1(b) is the $A/(d/2)$ plot for the same set of parameters. $A/(d/2)$ increases with thickness for higher temperature, and is almost constant over three orders of thickness, indicating a slope selection at

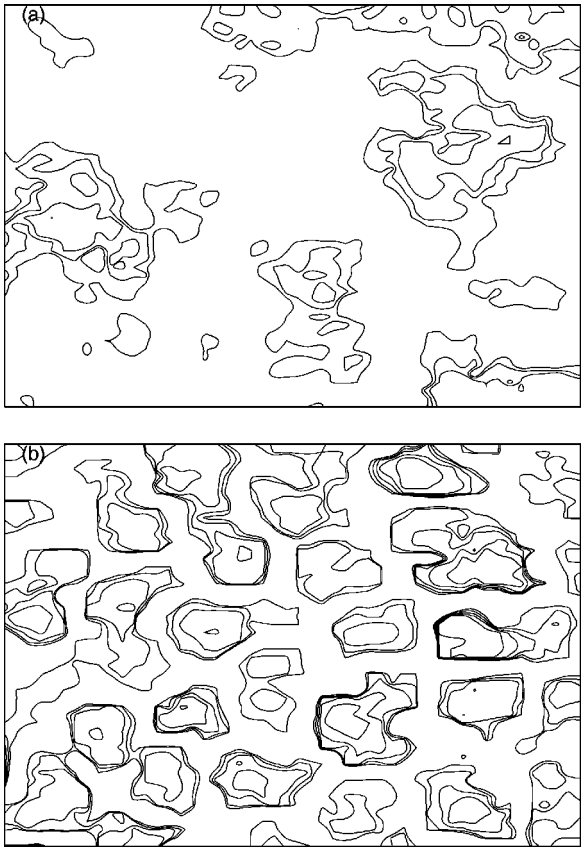

FIG. 2. (a) Morphology at lower temperature over a 100×100 region corresponding to the growth in Fig. 1. The number of layers grown is 10000 ML. The outermost contour is at 10002 ML, and is incremented in units of 2 ML. (b) Morphology at higher temperature. The number of layers grown is 2000 ML. The outermost contour is at 2005 ML, and is incremented in units of 5 ML.

lower temperatures. The average slope is $\approx 11°$. By controlling the downward bias for isolated adatoms, the upward bias for step attached adatoms, and n, slope selective growth with different average slopes is possible. Thus with $p_1=0$, $p_2=1.0$, $q=0.25$, $p_3=2.0$, $p_4=0.2$, and $n=2$, a growth with $\beta=0.18\pm0.02$ and an average slope of 13° is obtained, which resembles the growth on the Fe(100) substrate [4]. Thus a negative SESB provides the necessary downward current to balance the upward current for slope selection to occur. This may be an additional or substitutional process for funnelling.

Figures 2(a) and 2(b) show the contour plots for higher and lower temperatures. As expected, the low temperature growth forms wider and shorter mounds compared to the higher temperature ones growth.

Comparison with growth on Ge*(100)*: In this experiment [2], atomic force microscopy is used to study the surface morphology. Height-height correlation functions are obtained at different temperatures to deduce the amplitude A and base d as described earlier. For the sake of comparison we consider results at 155° and 100 °C. At 155 °C, A varies from 0.18 to 1.8 nm over a range of 5–200-nm thickness. At 100 °C, the variation is almost parallel but of higher magnitude. The slope in the range from 25–200 nm is close to 0.8,

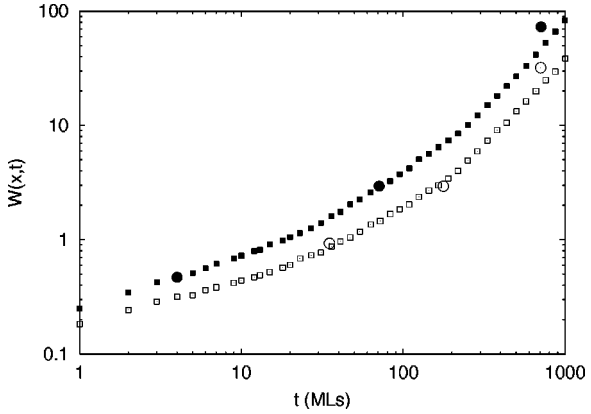

FIG. 3. Plot of w_2 vs thickness for $p_1=0.1$, $p_2=1.0$, $p_3=0.5$, $p_4=1.0$, $q=0.3$, and $n=80$ (open squares, high temperature), and for $p_1=0.07$, $p_2=1.0$, $p_3=0.4$, $p_4=1.0$, $q=0.2$, and $n=50$ (solid squares, low temperature). $L=200$ in both cases. Points plotted with larger symbols are from the experimental measurements taken from Ref. [2]. The thicknesses are converted to ML units, and lowermost values of $A^2/2$ are matched with simulation values of w_2 on the thickness axis. Other values are scaled accordingly. Open circles are values at 155 °C, while solid circles are at 100 °C.

while in the lower thickness range it is around 0.4. If the diffusion of isolated adatoms with positive SESB's is the only means of relaxation, then $\beta\leqslant0.5$. Thus simulations involving only this relaxation process are limited in explaining these observations. In Fig. 3, w_2 is plotted as a function of thickness for two sets of parameters. The expected qualitative behavior is clearly seen. The slopes are 0.4 ± 0.03 and 0.69 ± 0.05 in thickness ranges of 35–175 and 175–750 ML, respectively, at higher temperature. The equivalent range of monolayers is obtained by using the lattice constant for Ge, 5.65 Å, and noting that there are four layers within the lattice unit along the (100) direction. At lower temperature in the same range of thickness, these values are 0.45 and 0.68. In this case a value of n as high as 80 is required to keep the value of A reasonably low, as observed in the experiment. However, the experimental values of the mound base d are much larger than the ones obtained from the simulation. Values as high as 50 nm are obtained in the experiment at 155 °C, while the value is only 35 units (4.97 nm) from the simulation. The large d is indicative of large terrace diffusion as well as a low SESB [2]. It is possible to obtain a large d by tuning the parameters accordingly; however, the substrate size becomes too large to perform the simulation under such conditions.

Figure 4 shows the plot of $A/(d/2)$ for the two sets of parameters compared with 100 and 155 °C growth. Initially the ratio is constant, implying a slope-selection-like process. It increases later as observed in the experiment [2]. Finally, Fig. 5 shows the morphology of the surface grown after 1000 ML, corresponding to the higher temperature growth parameters. Low angled mounds are visible, along with the pits formed around them.

It is observed that in all cases where d tends to saturate, σ is negative, and keeps decreasing. The pits formed anchor the growth of the mound in that direction. Thus mound

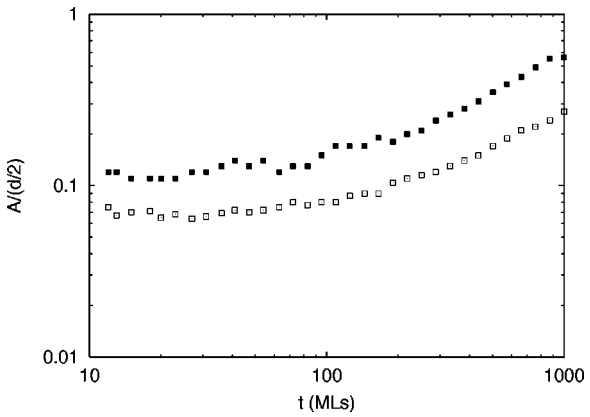

FIG. 4. Plot of $A/(d/2)$ vs thickness for the parameters used for producing results in Fig. 3. The symbols used to plot the curves in both, this figure and previous figures correspond to the same set of parameters.

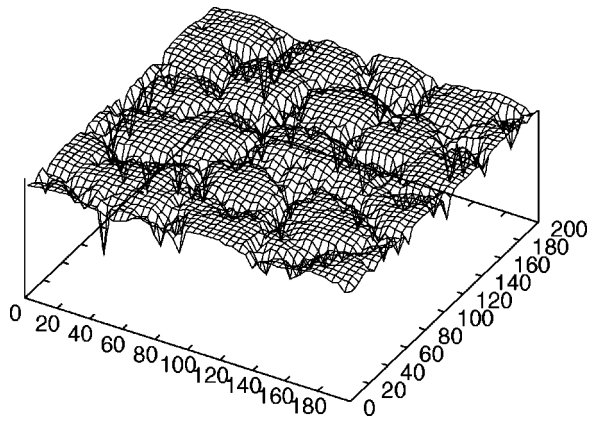

FIG. 5. Morphology of the surface after a growth of 1000 ML for the high temperature growth parameters used in Fig. 3. Note the pits on the surface. The high sloping walls around the pits are visible near the edges.

coarsening almost ceases when the pits completely define the boundary of the mounds. The depth of the pits grows with the thickness, causing a decrease in the value of σ. In the limit of large thickness, σ tends to saturate. When slope selection occurs, the kinetics is such that the pits are not permanently anchored on the substrate. Hence the mound coarsening continues. However, even in the limit of large thickness, the pits remain on the surface, leading to negative σ. These pits are ''angular points'' described in Ref. [10] for $1+1$-dimensions.

In conclusion, the time evolution exponent β for mounds is related to the type of hops involved in the relaxation of deposited atoms. Upward hops are necessary to obtain $\beta > 0.5$. A simple model incorporating these hops confirms this assertion. The model presented above is versatile in the sense that it can be adapted to describe the growth morphology of different materials. In most cases the surface is characterized by pits. The dynamics of pits decide the course of the mound coarsening.

[1] See, e.g., A.L. Barabasi and H.E. Stanley, *Fractal Concepts in Surface Growth* (Cambridge University Press, New York, 1995); Phys. Rev. E **53**, 359 (1996).
[2] J.E. Van Nostrand, S. Jay Chey, and D. Cahill, Phys. Rev. B **57**, 12 536 (1998).
[3] H.J. Ernst, F. Fabre, R. Folkerts, and J. Lapujoulade, Phys. Rev. B **72**, 112 (1994).
[4] J.A. Stroscio, D.T. Pierce, M.D. Stiles, A. Zangwill, and L.M. Sander, Phys. Rev. Lett. **75**, 4246 (1995).
[5] W.C. Elliott, P.F. Miceli, T. Tse, and P.W. Stephens, Phys. Rev. B **54**, 17 938 (1996), and references therein.
[6] M.D. Johnson, C. Orme, A.W. Hunt, D. Graff, J. Sudijono, L.M. Sander, and B.G. Orr, Phys. Rev. Lett. **72**, 116 (1994).
[7] J. Villain, J. Phys. I **1**, 19 (1991).
[8] M. Siegert and M. Plischke, Phys. Rev. Lett. **73**, 1517 (1993).
[9] M. Rost, P. Smilauer, and J. Krug, Surf. Sci. **369**, 393 (1996).
[10] P. Politi and J. Villain, Phys. Rev. B **54**, 5114 (1996).
[11] L. Golubovic, Phys. Rev. Lett. **78**, 90 (1997).
[12] S. Das Sarma and P. Punyindu, Surf. Sci. Lett. **424**, L339 (1999); S. Das Sarma, C.J. Lanczycki, R. Kotlyar, and S.V. Ghaisas, Phys. Rev. E **53**, 359 (1996), and references therein.
[13] J. Amar and F. Family, Phys. Rev. Lett. **77**, 4584 (1996); and Phys. Rev. B **54**, 14 742 (1996).
[14] P. Smilauer and D.D. Vvedensky, Phys. Rev. B **52**, 14 263 (1995).
[15] M.C. Bartelt and J.W. Evans, Phys. Rev. Lett. **75**, 4250 (1995).
[16] J. Krug, Adv. Phys. **46**, 139 (1997).
[17] J. Krug, M. Plischke, and M. Siegert, Phys. Rev. Lett. **70**, 3271 (1993).
[18] R.L. Schwoebel, J. Appl. Phys. **40**, 614 (1969).
[19] O. Pierre-Louis, M.R. D'Orsogna, and T.L. Einstein, Phys. Rev. Lett. **82**, 3661 (1999); M.V. Raman Murty and B.H. Cooper, *ibid.* **83**, 352 (1999); S. Das Sarma, P. Punyindu, and Z. Toroczkai, Surf. Sci. Lett. **457**, L369 (2000).
[20] M. Siegert and M. Plischke, Phys. Rev. Lett. **73**, 1517 (1994).
[21] J.M. Kim, M.A. Moore, and A.J. Brey, Phys. Rev. A **44**, R4782 (1991).